

SYNTHESIS REPORT

FOR PUBLICATION

CONTRACT No : **BRE2-CT92-0157**

PROJECT No : Project **BE5132**

TITLE : **CHARACTERISATION OF DISPERSIONS FOR PROCESS CONTROL IN THE PRODUCTION OF PARTICULATE MAGNETIC MEDIA**

PROJECT COORDINATOR : **BASF Magnetics GmbH**

PARTNERS : **Xidex (UK) Ltd.**
University College of North Wales Bangor
, **Keele** University

REFERENCE PERIOD FROM 1.11.92-31.07.96

STARTING DATE : 1.11.92 DURATION :45 MONTHS

PROJECT FUNDED BY THE EUROPEAN COMMUNITY UNDER THE BRITE/EURAM PROGRAMME

Characterisation of Dispersions for Process Control in the Production of Particulate Magnetic Media

Abstract

A vast majority of magnetic recording media is made by applying a magnetic ink containing elongated small magnetic particles to a flexible plastic substrate. In tape products it is usual to apply an orienting field to align the elongated particles in the recording direction and thus improve the magnetic properties of the tape. It is also essential that in addition to good magnetic properties the coating have a smooth and almost defect free surface, so a process of calendaring is always applied to 'iron' the surface flat. It is clear that the attainments of both good, **uniform**, magnetic properties and a smooth surface depend ultimately on the quality of the magnetic ink and the possible presence of large and small agglomerates. Despite the essential role played by the dispersion quality of the ink it has been traditional within the tape manufacturing business to apply only subjective and empirical interpretation to dispersion characterisation.

A Brite/Euram consortium of academic and industrial partners was formed to investigate methods to improve the art of magnetic dispersion characterization, generate new understanding and models of the behaviour of these systems and thereby to aid the efficiency of magnetic media production and expedite the development of new products. Many **experimental** techniques were evaluated. Of particular value have proven the methods of **magnetometry** in a shear field, analytical filtration techniques and the behaviour of the dispersions at short time scales in a newly developed pulse field magnetometer.

Concurrently with the experimental work a numerical simulation was developed with which to interpret the laboratory data and to become a design tool for media processing and development. Two separate models were developed. The first used Monte-Carlo techniques to generate equilibrium **configurations** of the particles taking into account magnetic and surface interactions. It became clear from both the simulations and the parallel experiments that **complex** time effects play an important **role** in the **behaviour** of the dispersions and true equilibrium situations may be **difficult** to find and may in fact not occur in *real* systems. The second model therefore adopted the molecular dynamics approach **while** taking over much of the framework of the Monte-Carlo calculation. With the molecular dynamic simulation good agreement has been achieved between the measured and calculated macroscopic magnetic properties of advanced metal particle dispersions. After incorporating a simulated '**drying**' stage the **model** can now generate numerical **model** of recording tape as the basis for fundamental recording theory.

Introduction

The assessment of the quality of magnetic dispersions is of great importance in the tape manufacturing industry. There is much wastage due to the fact that sub standard dispersions are often only detected once coating has taken place. There is also much loss of time in development work if every trial formulation must be made into a tape and evaluated in a recording test and the problem that mistakes in processing may cause false judgments about the quality of a dispersion. This is especially important for the development of future data storage products that will need to be **manufactured** to even tighter tolerances than current media. A dispersion consists of a magnetic pigment in one of three states; **single particles**, **aggregates** and **agglomerates**. Aggregates

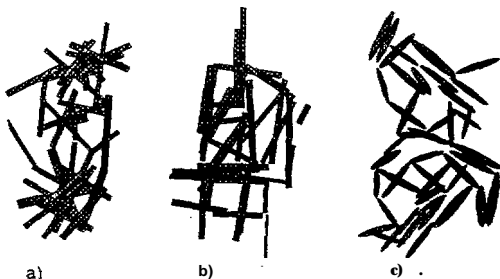


Figure 1. Some possible components in the magnetic structure of a dispersion: a) random agglomerates of varying sizes and some single particles, b) aggregates of particles at crystallographically preferred (in this case parallel) orientations, c) single particles.

are **tightly** bound collections of single particles (figure 1). The binding forces between the particles are large. As such any milling processes are unlikely to break down the aggregates. Agglomerates are more loosely bound single particles and aggregates and these may or may not be broken down by milling of the dispersion.

Preparation of Dispersion

Flexible magnetic media consist of a base film or web coated with a dispersion. The dispersion is a chemically complex system containing many different components, one or more of which are magnetic, which perform a range of **functions**. In order to study the magnetic properties of a dispersion an appreciation of the complexity of the system is needed, the

magnetic pigment is free to move around in the dispersion and does so if a magnetic field is applied. A typical dispersion will contain; magnetic **pigment**, wetting agents, **secondary** pigments, resins and lubricants in a suspension of one or more solvents. Pigments with a wide range of **coercivities** can be used depending on the potential application of the resulting media. The three most common pigment types are, in ascending order of **coercivity**; $\gamma\text{-Fe}_2\text{O}_3$, CrO_2 and Metal Particles. The wetting agents are **chosen** so that they coat the magnetic particles, enabling the solvents to wet the pigment. The **actual** properties of the wetting agent are **chosen** such that it bonds readily with the pigment surface. For $\gamma\text{-Fe}_2\text{O}_3$, which has an acidic surface, **surfactants** such as phosphate esters are used whilst for CrO_2 , which has a surface with an alkaline **nature**, materials such as **carboxylic** acids are often used. The amount of wetting agent used is minimised to prevent layers of tape from becoming sticky; the precise amount is determined in trials and must account for the presence of filler particles and **also** interactions between the resin and the **surfactant**.

Resins are of prime importance since they keep the pigment particles **separate** in the final coated product and also bind the dispersion to the web and hold everything together. The **resin** needs to be smooth and durable in order to resist wear **from** the **read/write** head, it must also be flexible, not crack and stay attached to the web. In order to achieve this two resin types **are** usually used. Typically, resin formulations are **proprietary** but most often consist of a mixture of hard and soft polymeric materials. By blending soft and hard resins it is possible to avoid the problem of sticky surfaces which occurs when hard resins are plasticised by the addition of lower molecular weight additives. The resins must also have the correct physical chemical relationship to the wetted pigment and substrate film in order to provide cohesion of the pigment and adhesion to the substrate. The resins must be **stable** over a range of environmental and climatic conditions **which** means the effects of hydrolysis, and other components of the dispersion must be taken into account. The resin must also be able to survive the manufacturing processes, such as **calendering**, from which high temperatures may result, there are also the high local temperatures which can result from head/media friction to be overcome.

The modern recording media contains polyurethane resins. These materials offer a wide range of physical properties such as high elongation at **break**, high modulus, high tensile strength and volatility in commercially available solvents together with a **high** glass transition temperature. The resins usually consist of block copolymers in which hard and soft segments are alternated down the polymer chain in order to give the required mechanical properties. In a typical example, shown in figure 2 there would be six to twenty repeat units of the hard, urethane, segment whilst the soft segments are **usually** polyesters. The resin molecules can combine to form a **para-crystalline** structure of non-regular parallel chains which has the properties of both a rubber and a resin.

A typical **flexible** media product will combine the urethane resin with a second, harder, resin such as vinyl, which can enhance the glass temperature of the system. Prior to coating the resins are cross-linked, this allows **solution** polymers of low molecular weight to be used during the dispersion process, reducing the risk of defects due to resin gels, but which are activated to form higher **molecular** weight chains by the cross-linking process. The **latest** approaches to using resins in dispersions are aimed at producing wetting resins which can substitute for some or **all** of the **surfactant** in the formulation. This is advantageous with modern pigments since the smaller particle sizes used today have a **large** surface area to mass ratio. Without wetting resins, a considerable fraction of the formulation would otherwise consist of **surfactants**, which can adversely **affect** the rheology of the dispersion and the resulting tape,

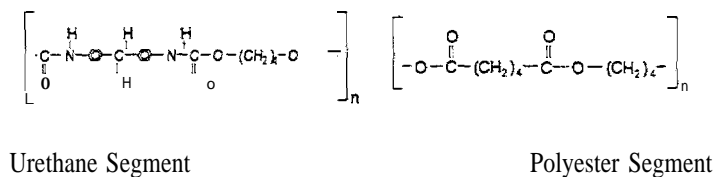


Figure 2: Hard and soft segments of a urethane resin

Further components added to the dispersion help to reduce static buildup on the tape, e.g. carbon black, and hence **allow** the tape to stack properly. **Carbon** black can also act as a lubricant and filler particle to allow smooth running of the tape. Sometimes abrasive particles such as **alumina** are added to **help** keep the **read/write** head free of debris and deposits removed from the tape. The abrasive particles are of a similar size to the magnetic particles and are added to the dispersion at the same time.

The final additives to the dispersion are lubricants, which control the friction and hence the wear of the tape. For tapes the lubrication is internal and is supplied by additives dissolved in the dispersion solvents. Silicone and other oil based lubricants are a common choice, these form a separate phase in the finished tape and provide for low head wear and good temperature resistance. However, these lubricants alone may give rise to frequency modulation noise and so lubricants compatible **with** the resin system are also added. These are usually surface active, fatty acid derivatives or maybe organic esters such as **butyl stearate**, **isocetyl stearate**, etc.

The first stage in the preparation of a dispersion is the premix. This has the objective of **blending** all the components together and allowing the **surfactant** or wetting resin to coat as much of the pigment surface as possible. In the case of metal particle dispersions in particular, the pigment and the wetting agent are kneaded together for several hours prior to mixing to form a high solids ratio paste which is then diluted to a slurry.

Once the premix or slurry has been prepared the next stage is to mill the dispersion, ideally this should produce a homogeneous dispersion which can be coated onto the base film. The milling process is also high shear, the mill is filled with zirconia beads which generate high tearing forces as they pass close to one another in the milling chamber. The dispersion is pumped through the mill and the agglomerates are broken down by the action of the beads.

Care has to be taken when milling not to put too much energy into the dispersion, as this can cause over milling and lead to broken particles which will widen the switching field distribution of the final tape. After milling the dispersion for a time the next stage of manufacture is the **letdown** process. This involves reducing the dispersion viscosity with the addition of extra solvent and resin solution prior to coating. Typically, the dispersion viscosity is reduced by 50% in the **letdown procedure**. The process has to be carried out **carefully** since if a **large** quantity of solvent is added suddenly it can induce flocculation of the pigment particles, a situation known as “solvent shock”. The solvent is always added whilst the dispersion is under high shear to help prevent this. The solvent is added slowly in several stages and the dispersion is filtered **afterwards** to remove any flocculates that may have formed.

Cross-linking of the resins is the **final** process before coating takes place. This maybe achieved by radiation curing or the addition of a cross-linking chemical. The amount of activator added to the dispersion must be **sufficient** to ensure that the reaction proceeds fast enough, such that long periods of storage under warm conditions are not required, but not so fast that the process has advanced too far before the calendaring is carried out. After coating and calendaring the final curing is carried out by storing the rolls of tape for several days at warm temperatures prior to slitting and packaging the tape.

During the dispersion preparation process it is usual to draw off small amounts and prepare hand samples for **gloss** measurements and **examination** under the optical microscope. These measurements detect gross agglomerates in the dispersion and are a proven way to monitor the progress of milling. However they say little or nothing about the fundamental state of agglomeration in the dispersion,

Therefore there is a wish for methods to **analyse** the dispersion in a more **scientifically** based way. The unique properties of magnetic recording dispersions make their characterization especially **difficult**. The particles are extremely small; the dispersions are concentrated and opaque, so that standard optical measurements are excluded, and even a ‘stable’ magnetic ink is not a stable colloidal dispersion in the normal sense. Magnetic recording particles are magnetic single domains magnetized to saturation and thus are **powerful** miniature permanent magnets. **Steric** stabilization cannot compete with the enormous magnetic **attraction** between the particles and magnetically bound flocs or secondary agglomerates will always **be** present in the ink in addition to **primary** agglomerates. An analysis of the dispersion must therefore distinguish between the permanent primary agglomerates, which are a defect of the dispersion and the unavoidable secondary agglomeration,

Technical description

Characterization measurements on dispersions are only of value if they have bearing on, and can be related to, the recording performance of a tape made with that dispersion. Consequently the bulk of the experimental effort was devoted to preparing dispersions by various means and with various components, measuring these dispersions with a range of techniques, coating and measuring tape, and subsequently seeking relationships between the measurements. From these experiments three methods have shown the most promise.

Shear magnetometry

As described in the introduction% because of the inevitable magnetically induced flocculation a **monodisperse** system and one containing agglomerates look very similar in the stationary state. An important step forward in distinguishing the two states was taken by **Scholten** [refs 1-3] who introduced shear energy in order to breakup **temporary magnetostatically** bound structures. **Scholten’s** original apparatus was restricted to shear rates of 200 S⁻¹ and an applied field of 100 kAm⁻¹. We have refined and developed this technique to a routine laboratory measurement and extended its range to coverall current types of magnetic tape dispersion,

The key was to develop a shear cell which was easy and reliable to **use**. This took several generations of development.

The present construction of the shear cell is shown in figure 3. The liquid to be measured is injected with a syringe into the space between the **stationary** outer wall and the rotating cylinder. Small glass spheres are then used to seal the filling and air escape holes. A sliding coupling provides the drive **connection** between the vibrating cell and a stationary electric motor. The **cell**, pick-up, and **field** coils of the magnetometer are **all**

co-axial. Because there is some dead space at the ends of the sample volume, the pick-up coils are designed to have zero sensitivity there. **Stable** operation is **achieved with** rotation speeds up to 6500 rpm, which combined with a gap of 0.1 mm gives a maximum shear of approximately 13000 s^{-1} , but for **standard** measurements 4000 rpm and a 0.5 mm gap are **chosen** to extend the **life** of the bearings and seals and for a stronger magnetic signal. At the centre of the sample the effective demagnetizing factors of the two geometries are 0.0017 and 0.008, and comparative measurements with the two **cells** have shown their effect to be negligible, The same cell is used for static measurements without shear and dispersions which display instabilities can be sheared for a short time before the measurement in order to **restore** then to a well defined state.

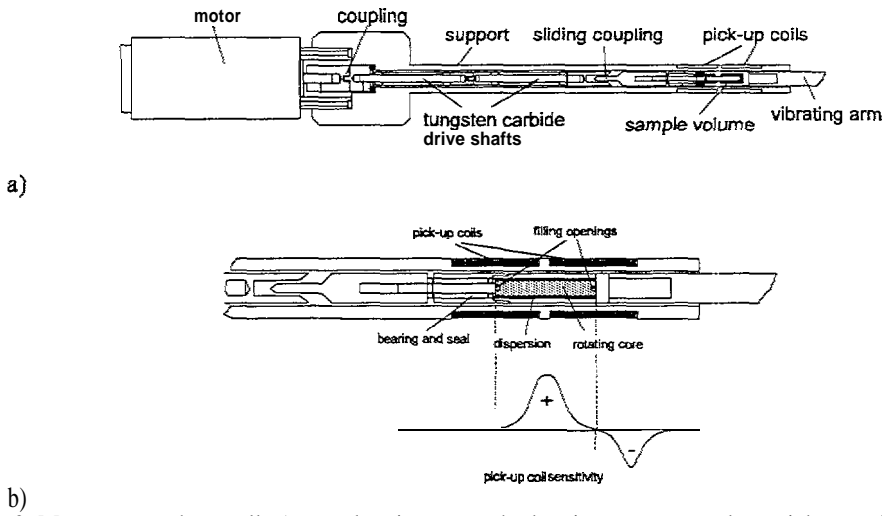


Figure 3. Motor driven shear cell. a) The electric motor, the bearing support, and the pick-up coils are mounted on the movable field coils of the magnetometer. The sample cell is mounted on the vibrating arm. To engage the sliding coupling between the two parts, the field coil is moved carefully over the vibrating arm while the motor slowly rotates. b) Details of cell showing filling apertures. The dispersion is injected through one opening while air escapes from the other. In this way air bubbles in the dispersion can be avoided. The openings are then sealed with small glass spheres. The geometry of the system is chosen so that the dead space to the right of the rotating core, and the ill defined region near the bearing on the left are in regions of very low sensitivity and do not contribute to the magnetic signal.

A typical measurement involves sweeping the applied field in the VSM first from zero to 380 IcAm^{-1} and back to zero (legs 1 & 2 of the measurement in figure 4), then repeating the sequence for negative fields (legs 3 & 4). A geometrical sequence of field steps is used to increase resolution in the low field region. When very high shear is applied fewer points are taken so as to limit the possible temperature rise of the sample during the measurement, The few cases where large temperature increments were observed turned out to be the result of incorrect assembly of the cell and heating of the sample has not proven to be a general problem

Results of measurements on a simple iron oxide formulation are shown in figures, 4 and 5. In the stationary liquid, irreversible magnetization processes continue up to 100 kAm^{-1} and the susceptibility peak on the initial magnetization curve spreads well past the powder coercivity of 26 kAm^{-1} . This could suggest that much of the magnetization process involves particle switching in primary agglomerates. Sheared, however, the magnetization behaviour is quite different. The area A_H between leg 1 & 2 of the normalized magnetization curves is very small and no hysteresis can be observed above 30 kAm^{-1} . The sample is in fact very well dispersed. Because A_H is of course dependent on the particle coercivity a new number Φ is defined by normalizing AH to the powder coercivity to give a parameter for of the fraction of material that cannot be magnetized by free rotation and must be switched irreversibly. Φ is a measure of the degree of dispersion and has indeed been found to correlate with the quality of the tape prepared from the dispersion. The actual value of Φ depends on the nature as well as the number of agglomerates, The irreversible magnetization is due to reversal of the remanence, consequently for a dispersion consisting entirely of large, random, initially demagnetized, agglomerates $\Phi \approx 0.5$. For pairs of identical parallel but oppositely magnetized particles $\Phi \approx 1$, while it is obviously zero for a perfectly dispersed system. Φ can also be zero for orthogonal pairs of particles, a case which is unlikely to occur, but which demonstrates the need for a further dispersion parameter, the orientability as measured by the relative remanence (squareness) of the dispersion, In the preceding examples the perfectly dispersed system has a potential squareness of 1 while that of orthogonal pairs of identical particles is only 0.7, clearly distinguishing the two cases. In the static measurement the relative remanence sq_r after saturation is an indication of the tape squareness to be achieved with a coating line with a single orienting magnet, it may not, however, be a good parameter for the true orientability of the dispersion. If the dispersion

were instead to be frozen in a high applied field then the resulting maximum possible squareness sq_{max} would be limited by the number of particles in non-parallel agglomerates. In the liquid state magnetostatic forces tend to rotate the particles as the external field is removed, thus reducing sq_r below sq_{max} . Information about sq_{max} is contained in the high field approach to saturation of the magnetization. In a perfect dispersion this part of the curve should be essentially flat and a linear extrapolation back to zero field would give $sq_{max} \approx 1$. For real dispersions a better extrapolation is needed. Empirically, an exponential function of the form $1 - \beta e^{-\beta/H}$, fitted to the portion of the descending magnetization curve above 200 kAm^{-1} was found to predict the squareness of tapes, i.e. 'frozen' dispersions, very well, figure 6, and has been used to calculate sq_{max} . How much leg 2 of the measured curve deviates from extrapolation depends on how well dispersed and mobile the particles are. The point at which the two curves separate is a guide to the strength of field required to prevent disorientation of the dispersion by self demagnetization.

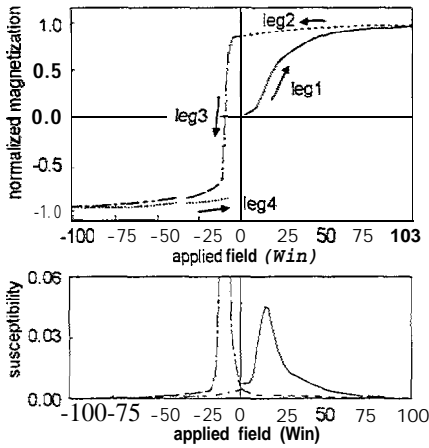


Figure 4. Normalized magnetization and susceptibility measured without shear on a $\gamma\text{-Fe}_2\text{O}_3$ tape dispersion. The powder coercivity is 26 kAm^{-1} . The measurement starts at zero field with a freshly prepared sample. The arrows and leg numbers indicate the sequence of measurements.

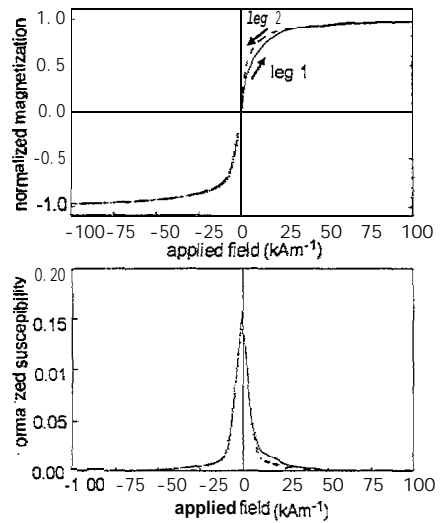


Figure 5. Same $\gamma\text{-Fe}_2\text{O}_3$ dispersion as figure 4 measured under shear.

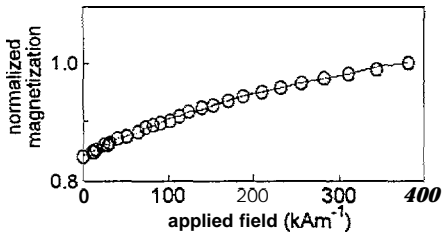


Figure 6. Extrapolation to the remanence of a tape sample from the high field magnetization. Circles are measured points on the descending magnetization curve (leg 2), continuous line is the extrapolation function fitted using only the data taken above 200 kAm^{-1} .

MP dispersions have behaves rather differently. Based on the \odot and sq_{max} criteria and confirmed in tape, it appears impossible to prepare highly dispersed MP dispersions solely by milling and a process of kneading is required as the first stage of dispersion. Kneaded dispersions pack better in the tape coating, and kneading has been described [ref 4] as a process of compacting of particle aggregates, The first conclusion from the measurement on a good kneaded dispersions is that kneading,

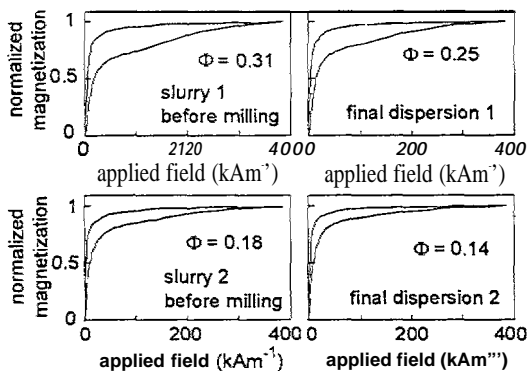


Figure 7. Comparison of slurry and final dispersion, after additional 10h of milling in a paint shaker, for samples kneaded with different powder to binder ratios. The final dispersion quality is already determined at the slurry stage.

Figure 7 shows the most important results obtained for MP. Two kneading experiments were performed and both the slurries and the final dispersions were measured. This result has both positive and negative aspects. On the one hand the changes observed during the milling of a good dispersion are so small that it is impossible to monitor the progress of a kneaded dispersion in this way. On the other hand, previously the only good test of a kneading or slurry preparation has been to coat and measure a tape. Our results now show that, at least for development purposes such as testing formulations or improving the kneading process, the slurry can be evaluated directly thus saving the work of milling and coating for the unsuccessful formulations.

By calculating the potential squareness and remanent moments for random agglomerates, of different size it is possible to set some limits on the nature of the agglomerates in a dispersion. sq_{max} is given by the average saturation remanence while, following [ref 3], two possible starting conditions are considered for the estimation of Φ . The agglomerates can be optimally demagnetized (relative remanence = r_d), or the particles they contain can be randomly magnetized (relative remanence = r_r). It can be supposed that large agglomerates will have grown in a demagnetized state during the powder manufacture, but that smaller agglomerates produced by subsequent dispersing of the powder will tend to be randomly magnetized. Φ is approximately the irreversible change in remanence between the initial and saturation remanences. The two values of Φ for demagnetized and randomly magnetized agglomerates are $\Phi_d \approx sq_{max} - r_d$ and $\Phi_r \approx sq_{max} - r_r$. The parameters sq_{max} , Φ_d and Φ_r have been calculated numerically by summing randomly generated agglomerates of particles with a lognormal size distribution and spatially random orientation and are plotted in figure 8.

Using figure 8 we can begin to interpret the magnetometry data further. Good kneaded dispersions of MP typically have sq_{∞} in the range 0.9-0.95 and Φ of 0.1 to 0.15. Remembering that Φ_r is more applicable to small agglomerates, a dispersion of two particle agglomerates could fit this range of parameters, but, as a distribution of agglomerate sizes is to be expected, a more satisfactory model is of a kneaded dispersion containing a substantial number of single particles with an admixture of agglomerates. For an optimal dispersion with sq_{∞} of 0.98 and Φ of 0.02, for example, there is little ambiguity, only a majority of single particles in the dispersion can fit the data. The sq_{∞} and Φ of laboratory dispersions prepared without kneading can typically be in the ranges 0.84-0.92 and 0.37-0.42 respectively. These large values of Φ require that a large part, perhaps all of the particle are to be found in agglomerates. It becomes easier to fit the high experimental sq_{max} value if lower angles between the particles are more common than in the random orientation model.

Analytic Filtration

The filtration of dispersions is a production necessity in order to remove at successive process stages any solid contamination or undispersible clumps from the suspension. Its control is crucial to low error rate performance of the finished product and the maintenance and replacement of filters is a significant cost item.

The material collected on a filter is indicative of the state of dispersion, inadequate levels of dispersion resulting in more rapid blocking of the filter bed. It therefore offers a method for dispersion characterisation.

Any method which is to be suitable for at-line manufacturing quality control must be simple, rapid in use, safe, and capable of use and interpretation by semi-skilled personnel. Such a method has been developed at Anacomp and has been tested extensively both in production over a substantial period of time and in the laboratory development of processes for new products, and their subsequent first production.

In order to meet the criteria the filtration set-up has to be such that significant blocking does occur with small quantities of dispersion over short time periods, ensuring that the flow curve of rate of passage of the filtrate

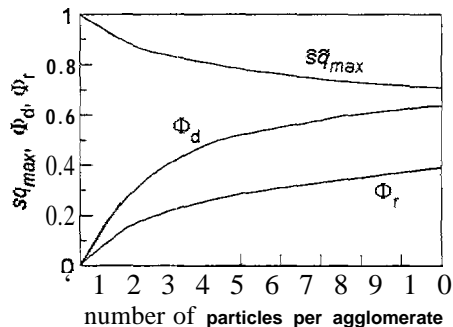


Figure 8. Calculated maximum squareness sq_{max} and hysteresis parameters Φ_d and Φ_r of random agglomerates as a function of the number of particles per agglomerate. A typical standard deviation of the particle volumes of 0.8 times the mean has been assumed.

has measurable curvature. The theory for calculating characterizing quantities from such curves has been evaluated and checked by experiment.

An extensive **programme** of tests was carried out to determine the optimum conditions for measurements relating to magnetic dispersions of various pigments and binder compositions. The chosen method is that 400 ml of the dispersion under test are placed in a vertically mounted cylindrical column, at the bottom of which is a polypropylene membrane filter of suitable nominal pore size. It was found for example that for a chromium dioxide data tape dispersion a very suitable pore size was 5µm : **optimum** pore sizes must be established experimentally for other formulations to adapt to the differing theories of alternative systems.

The top of the column is sealed and an air pressure, optimised by experience for the chromium dioxide formulation at one atmosphere over ambient pressure, is applied to it at zero test time. A container below the **filter** exit collects the filtrate on a **scale** pan, and the weight of filtrate is measured every ten seconds for a total elapsed time of up to 200 seconds, from which data the flow versus time curve can be plotted, and the required characteristics determined.

This operation can be carried out **manually**, or, where **safety** permits, by the use of an electronic balance feeding data to either a computer or to a PROM programmed microcomputer, giving a direct read out of the characterizing numbers for the **sample** dispersion. The first three readings are to be ignored in calculation, representing a 'bedding in' time for the membrane to stabilise under the first flow.

The equipment is relatively simple and reproducibility of results was found to be excellent and a problem only in one respect - that of reproducibility of the filter membranes themselves, the membrane being of course replaced after each test. It was determined that, with membranes from a reputable supplier, the reproducibility of them within one package was more than adequate for the purpose, **but** that a new batch required a small calibration correction to be applied, characterizing the filter batch itself. The precautions should be taken of avoiding 'just in time' membrane supply and of **pre-checking** the correction needed for each new batch ahead of using up the current supply.

There is extensive literature on filtration theory but this normally consists of curve fitting the flow curves by using simple mathematical models such as polynomials or exponential functions of an apparently empirical nature [refs. 5,6 and references therein]. **Anacomp** have made use of a more fundamental approach by deriving a fitting function which gives rise to only two characterizing numbers, based on the **Kozeny-Carman** theory of permeation of fluids through beds of particulate material [ref 7] which a **filter** membrane equivalences.

The rate of flow of fluid Q' through a porous mass of area A and thickness L under a pressure difference of P

$$\text{is given by the equation :- } Q' (\text{volume / time}) = \frac{P}{L} \cdot \frac{A \varepsilon}{\mu K} \cdot \frac{\varepsilon^2}{S'^2 (1 - \varepsilon)^2}$$

where P/L is the pressure gradient across the filter, A is the geometric cross-sectional area of the membrane, ε is the porosity of the filter bed, μ is the fluid viscosity, S' is the specific area of solid/fluid interface per unit volume of filtration medium solids, and K is a '**tortuosity**' factor to take into account that the flow paths through the bed are **labyrinthine**.

The terms P , L , and μ are constants of the **system**, given that the viscosity of the production materials under test is controlled to be constant. Should that not be the case, then a correction for the viscosity must be made. S' is invariant provided that blocking does not approach **completion**, as it will not with such small volumes of material passing through it. K is a **function** of the filter bed composition, absorbing also some numeric constants from the **Kozeny-Carman** theory. It depends chiefly on the degree of **fibre** orientation in the filter pack and may **also** be taken as constant, provided that the porosity is < 0.9 , above which value the assumptions of the theory break down. The porosity ε will decline if the filter bed pore channels themselves become constricted by retained material, a situation which is again unlikely with the relatively large filter pore size in comparison with the size of **particle** clusters and aggregates and with the limited amount of material which is in total collected. The effective area A will decline if the **orifices** of pores or their channels are blocked.

On the simple assumption that **only** A is varying from its initial **value** A_0 by reason of blocking of surface

$$\text{orifices by poorly dispersed material, then:- } A = A_0 - k \cdot \int_0^t Q' \cdot dt$$

where k is a constant in terms of the filter and of the fluid.

Applying the initial conditions that $Q(t=0) = 0$ and $Q'(t=0) = Q'_0$, the particular solution becomes :-

$$Q(t) = Q'_0 t e^{kt}$$

The terms Q'_0 and K are the characterizing parameters. These parameters are readily derived from the experimental flow curves, an example of which is shown in **figure 10**.

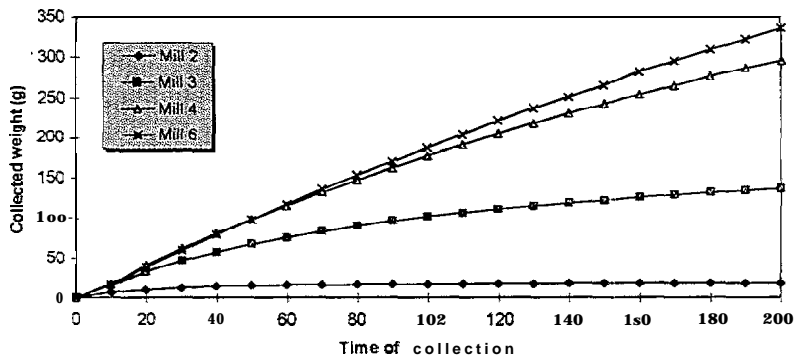


Figure 9 Experimental Flow Curves for Chrome Dioxide Dispersions, Letdowns prepared from Mill Slurries

An example of the experimental flow data fit to the theory is shown in the figure 11. Examination of the bed of residues during tests showed that the major factor in reducing flow is **not** the blocking of orifices to reduce the value of A , but is a decrease in the pressure gradient due to build up of the bed of material on the surface, and that it is the initial formation of this bed which is chiefly responsible for the starting up stabilisation period. Since both P/L and A are linear multiplying terms in the equation and are subsumed in K , the final equation above remains unaffected.

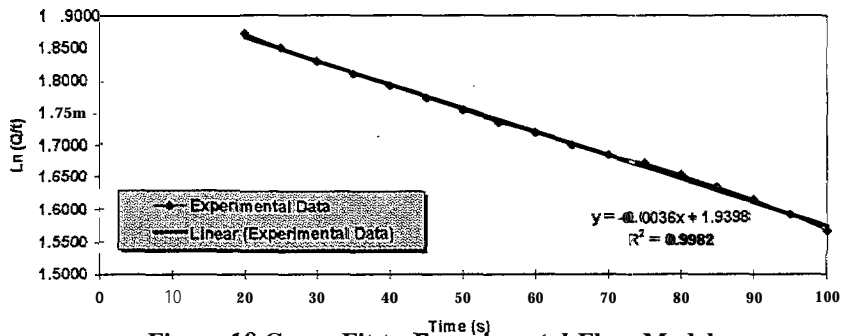


Figure 10 Curve Fit to Experimental Flow Model

Correction factors where needed can be applied to the parameters K and Q . Experience has shown that for general purposes it is sufficient to make a viscosity correction by use of the value obtained by rotational viscometry, such as that routinely taken in the course of process control. For more precise work in laboratory and in process development the viscous modulus as determined by oscillatory rheometry is preferred.

Initial tests showed that the two parameters monitored the progress of a dispersion very satisfactorily. For example, taking partially dispersed chrome dioxide material from each of the successive milling stages of a production line and diluting each to a ready-for-use condition in the laboratory, the following results were obtained - figure 11.

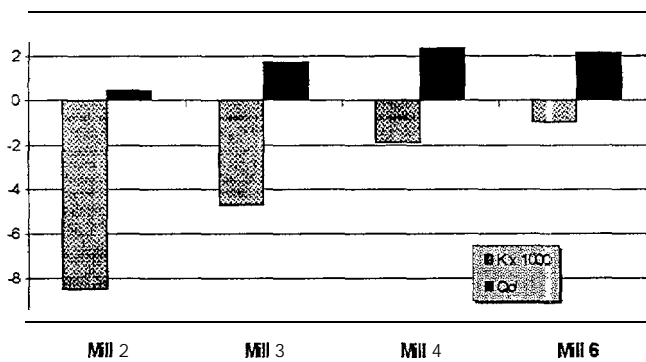


Figure 11 Filtration parameters for CrO_2 dispersions

Following this preliminary work and many confirmatory evaluations the method was used to monitor the production of chrome dioxide dispersions on the factory floor sampling daily over a period of three months. During this period two different chrome dioxide pigments were used - one type supplied by a European vendor, the other was USA sourced.

Table 1 summarises the results for fifty filtration evaluations and compares these with ‘dispersion grades’ given by the Process Control Laboratory.

Table 1. Filtration parameters of production chrome dioxide dispersions.

Pigment Type	Q'_0			K			Dispersion Grade		
	n	\bar{v}	s	n	\bar{v}	s	n	\bar{v}	s
Type A	27	1.85	0.20	27	12.8	2.1	27	2.0	0.4
Type B	23	1.67	0.19	23	14.1	3.7	23	2.5	0.3

Of the two parameters K is the more sensitive but Q'_0 (actually reported as $\ln Q'_0$) is the more statistically stable. There is a statistical difference in the dispersion quality of the two pigments. Type A is the better by virtue of a higher Q'_0 and lower K value. This is confirmed by the dispersion grade following optical microscope evaluation. (Slides are graded on a 1-5 basis with 1 being the best dispersion grade). These results illustrate however the sensitivity of the filtration test method.

When a new product is involved for which process development is needed and which requires support *cm the* learning curve of product and process development and during first manufacture, and it is here that the filtration characterisation method has proved to be invaluable. In developing a new media. Filtration testing was of immediate and very real use.

It was necessary to rebalance the method to accommodate not only the different pigment but also the different functional resins which were employed. The pore size of the membrane, the applied air pressure, and the calibration corrections were re-optimised, and ‘viscosity’ correction was done by rheometry.

This newly developed characterisation method was particularly useful in working the product and its associated processes up into successful first production, since prior experience in slide assessment was by definition lacking.

Impulse Magnetometry on Dispersions

The major part of the development work at UCNW was taken up with the design and construction of a Pulsed Field Magnetometer (PFM). Figure 12 shows a block diagram of the system. The field is generated in two coils, each consisting of four strands of wire carrying the current pulse and a fifth strand which acts as a pick-up coil. The sample is placed in one of these coils and a bridge balancing network is used to cancel the change in flux common to both coils due to the pulsed field. The remaining signal is due to the change in flux of the sample. This signal is processed using an instrumentation amplifier, a variable time constant gated integrator and a compensation stage. This allows the change in voltage detected by the pick-up coil to be output as a signal representing the change in magnetisation of the sample.

The change in magnetisation is monitored on a Tektronix TDS640 500 MHz, 2 Giga sample per second digitizing oscilloscope. This enables us to monitor the change in magnetisation in real time, giving an effective picture of the state of the magnetisation under the pulsed field.

Some sample pulses produced by the system are shown in figure 13. The pulses shown are of 50 μs duration with rise and fall times of 2 μs . The pulses are free from overshoot and ringing and the maximum field amplitude is maintained without falling off throughout the duration of the pulse, indicating that the capacitive storage bank is sufficient to maintain the desired current level.

The pulsed field magnetometer can be used for measurements of magnetization and remanence curves. Figure 13(a) shows the procedure used to obtain IRM curves for the case where the applied field is less than that required to saturate the sample, H_{sat} . The

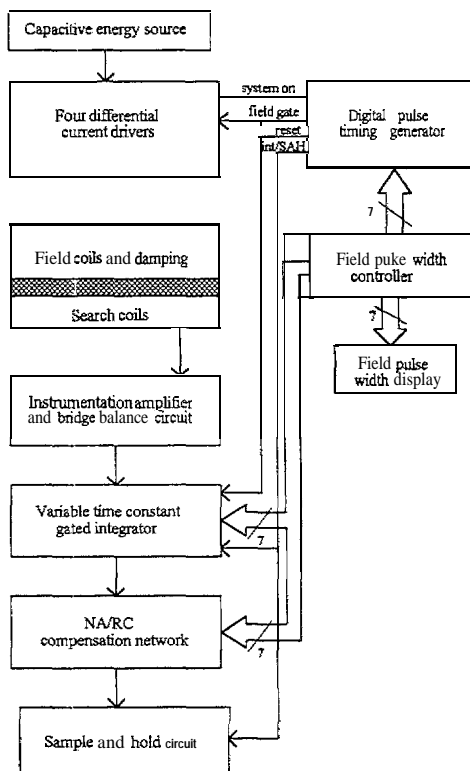


Figure 12 Pulsed field magnetometer system block diagram

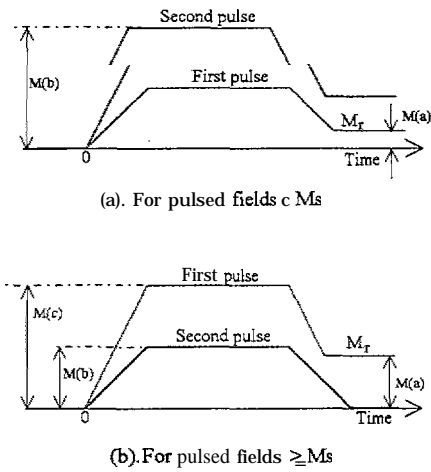


Figure 13: IRM measurement technique using the PFM

The remanence ratio is now simply $M_r/M_s = M(a)/M(c)$. Subsequent pulses will give a peak amplitude of $M(b)$ which will be equal to $M(c) - M(a)$ and will have no remanence.

Pulsed Field Measurements: Some responses of a $\gamma\text{-Fe}_2\text{O}_3$ premix dispersion to pulsed magnetic fields of $100 \mu\text{s}$ duration are shown in figure 14. The magnetisation appears to follow the applied field puke and no time dependent effects are visible. The remanence increases with field as expected and is always below the Stoner-Wohlfarth value for a randomly aligned system of particles of 0.5.

The response of a CrO_2 dispersion sample to a pulsed field is shown in figure 15. In contrast to the measurements with the $\gamma\text{-Fe}_2\text{O}_3$ dispersions, with the CrO_2 there is a slight lag of the magnetisation behind the applied field pulse both when the field is applied and when it is removed. The possible explanations for this are; particle rotation, magnetic viscosity effects or switching speed limitations. We can rule out magnetic viscosity effects since measurements on frozen samples reveal that this effect is negligible in zero field. Motion of particles following magnetisation of the dispersion is a possibility. There are sufficient magnetostatic forces in a magnetised dispersion to initiate particle rotation. However, these effects are usually manifest over much longer time scales than the effects seen here. Thus, we can postulate that there is a switching speed limitation in some of the particles in the dispersion, resulting in the time lag. This could perhaps be related to the particle size distribution in the dispersion.

Figure 16 shows some DCD curves of CrO_2 dispersions measured with the VSM and PFM. The curves shift to the right with milling time, We can explain this by considering the microstructure of the dispersion. A dispersion containing a large fraction of material that can rotate will be aligned to a greater extent by the saturating field applied before the DCD measurement than a dispersion containing lots of big aggregates and agglomerates. Well aligned samples will have a higher remanent coercivity than poorly aligned ones, therefore, the results in figure 16 lead us to conclude that milling samples for a longer time results in them having a larger fraction of particles able to rotate. This measurement may be used to discriminate between dispersion samples of different quality.

theoretical magnetisation responses to two pulsed fields are shown. For each point on the IRM curve two pulses are required. The first pulse is of magnitude H , this results in switching of some fraction of the magnetisation of the dispersion into the applied field direction and when the puke ends there is a remanence, $M(a)$. Subsequently a large puke, H_{sat} , sufficient to saturate the dispersion, is applied. We take the peak value of magnetisation induced by the second pulse to be $M(b)$. The saturation magnetisation of the sample is, therefore, $M_s = M(a) + M(b)$, since the fraction of the dispersion reversed by the first pulse is already magnetised along the applied field direction and will not contribute to the response due to the second pulse, The remanence ratio is thus $M_r/M_s = M(a)/(M(a) + M(b))$.

In the case where the first pulse is sufficient to saturate the sample then we have the situation shown in figure 13(b).

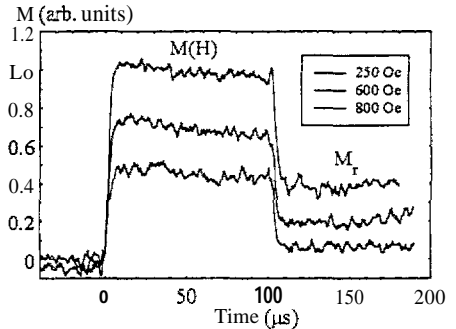


Figure 14 Response of a $\gamma\text{-Fe}_2\text{O}_3$ dispersion to pulsed fields of various amplitudes

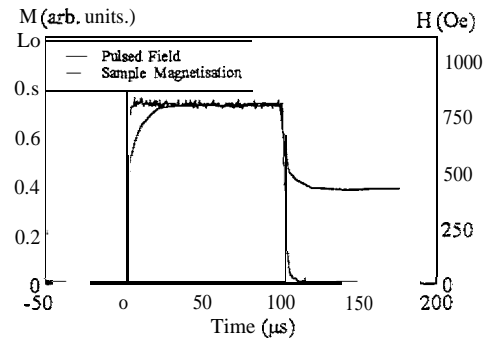


Figure 15: CrO_2 dispersion response to a pulsed field

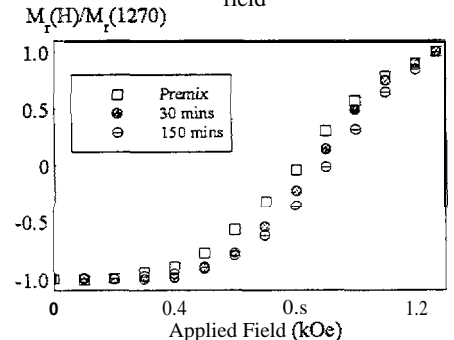


Figure 16: CrO_2 dispersion DCD curve

The response of MP dispersions to a pulsed field is shown in figure 17. The behaviour seen in the CrO_2 dispersion is repeated with the MP dispersion in that the magnetisation lags behind the applied field pulse although here the effect is much more exaggerated. We see the remanence increases with increasing applied field and also increases with milling time, albeit to a very small extent.

Figure 18 shows a magnetisation curve and remanence curve for a MP pigment sample. The increase in both the magnetisation and the remanence with applied field is linear and the sample is clearly not saturated by the largest applied field available on the PFM. The signal levels from dispersion samples of MP were very low, probably due to the low percentage of the material that could be switched by the available fields. The signal levels were too low to enable measurement of an MP dispersion IRM curve. However, a DCD curve was measured, for the DCD measurement the signal level is typically twice that of the IRM measurement because in the DCD measurements the sample is initially aligned whereas for the case of the IRM measurements the sample is not.

In view of the shapes of some of the magnetisation responses to the pulsed fields we studied the effect of varying the pulsed field width on the remanence ratios of dispersions. Field pulse widths of $5 \mu\text{s}$, $33 \mu\text{s}$, $66 \mu\text{s}$, $100 \mu\text{s}$ and $27 \mu\text{s}$ were used with a maximum field amplitude of 1270 Oe. The remanence ratio was found to increase with milling time with the largest increases being between the premix and the 15 minutes mill stage. The variation of M_r/M_s with pulse width is less dramatic with a slight upwards trend in M_r/M_s with increasing pulse width. For CrO_2 the values of M_r/M_s correspond well with those measured on the VSM. From the shape of the CrO_2 magnetisation response to the pulsed field we would expect a more significant change in M_r/M_s with pulse width and this is exactly the case. There is an increase in the remanence ratio with pulse width. The largest change in M_r/M_s with pulse width was found in the MP dispersion. With pulse widths above $60 \mu\text{s}$ the remanence ratio increases sharply.

Assessment of Dispersion Quality using Pulsed Field Magnetometry : The PFM was taken to Anacomp Data Products Ltd whereby it was used to carry out a set of measurements to enable the feasibility of using the instrument as an on-line quality assessment tool to distinguish between the premix, vertical milling stages, letdown, polishing, final filtering and activation states of a commonly used magnetic tape dispersion to be assessed. The dispersion studied was that used to prepare IBM 3480 tape for mass storage of data.

The experiments were carried out with the dispersion sample in a random state before application of the field pulses, hence a new sample was used for each field measurement. Five stages of the dispersion process were examined in this experiment, these were the premix stage followed by four milling stages. The pulse duration was kept constant at $90 \mu\text{s}$ and two fields of 832 Oe and 1069 Oe were used. These fields were chosen since they were found to be the fields where the most change could be detected. The Table summarises the findings from this experiment.

Process Stage and test Field (Oe)	First Pulse Remanence $M(a) M_r$	Maximum Magnetisation $M(b) M_{\text{max}}$	Remanence Ratio M_r/M_{max}
832- Premix	0.064	0.176	0.364
832- Vertical Mill 1	0.0060	0.180	0.333
832- Vertical Mill 2	0.056	0.172	0.325
832 - Vertical Mill 3	0.052	0.172	0.302
832 - Vertical Mill 4	0.048	0.161	0.298
1069- premix	0.092	0.152	0.605
1069- Vertical Mill 1	0.108	0.180	0.600
1069- Vertical Mill 4	0.084	0.156	0.538

Table Results for the premix and various stages of the milling process

From these results it was found that at a pulsed field of 832 Oe, the magnetisation reduces from the premix stage to the first milling stage to 91. 5% of that at the premix stage, to 89% after mill 2, to 80% after mill 3 and finally to 79% after mill 4. For the pulsed field of 1069 Oe it was found that the magnetisation reduces from the premix stage to the first milling stage to 99% of that at the premix stage, with a further reduction from the

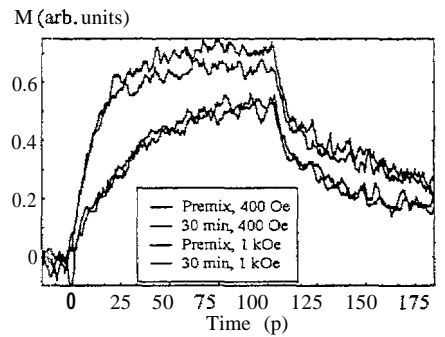


Figure 17: MP dispersion responses to pulsed fields

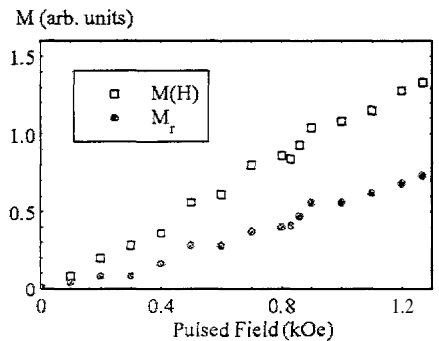


Figure 18: Magnetisation curves for metal particle pigments

premix stage to the fourth stage to 88%. There were no observable changes between the other milling stages and the premix stage using this field.

These results imply that the aggregates of particles are arranged in flux closure configurations, making it more difficult to switch particles. However, as dispersion proceeds and the aggregates are broken, it is easier to magnetise the particles in 832 Oe. At 1069 Oe, the field is large enough to reverse the particles in the aggregates. This means that non-saturating pulsed fields could be used as a measure of dispersion quality.

Mathematical simulation of magnetic dispersions

Before being able to extrapolate the results of the magnetometry and time dependence measurements in the design of new systems a quantitative model is essential. Therefore a large effort was devoted to establishing such a model, based first on Monte-Carlo and later on molecular dynamics algorithms,

The Monte-Carlo model The Monte-Carlo technique is statistical rather than mechanistic. That is we consider the properties of a system made up of many classical particles rather than the behaviour of the individual particles. Our fundamental consideration is the equilibrium distribution, not the equations of motion of the particles. The Monte-Carlo method is derived from the theory of the finite and stationary Markov Chain which may be employed to generate a set of random variables that conform to a steady state distribution.

It was also found that it was difficult to obtain a realistic configuration for the system at high densities, due to problems arising from the particle geometry and the volume density of the ensemble. Such problems were avoided by creating a low-density system using the random placement technique and then by allowing the particles to expand up to their full length and to the correct packing density. During the expansion procedure the interactions were gradually scaled up and by this route it was found possible to produce realistic initial configurations which, in conjunction with the force bias Monte-Carlo method, evolved towards the equilibrium state within a realistic computer time.

In all calculations the particles were modelled as circular cylinders with spherical end caps. For detailed comparison with experimental measurements the best available data on particle size distributions and magnetization were provided by the industrial partners.

The simulation is conducted within a cubic computation cell. The cell represents a typical small volume of the bulk dispersion. The particles in the cell are assumed to be free of any surface effects of the bulk material. Particles are free to leave the cell through any of the bounding surfaces but are simultaneously replaced by a particle entering the cell from the opposite side. The particle entering the cell is an exact image of the particle leaving. This image is repeated every cell length in directions perpendicular to the cell sides. Thus the use of periodic boundary conditions imposes a periodicity on the particle configuration which is determined by the size of the cell. This results in a symmetry being imposed on a bulk material which should really be isotropic. Computer resources limit the number of particles in a cell the practical limit was 1000 particles exhibiting a packing fraction of $\approx 10\%$.

The magnetostatic interactions are approximated by a magnetic pole sited on the particle axis at the centre of each hemisphere. The strongest interaction between the particles is the short range effect of the surfactant layer. The layer tends to prevent particles adhering together in surface contact under the attractive van der Waals and London forces, The surfactant also provides a repulsive potential between particles in close proximity which assists the dispersion processes and resists flocculation. The effect of the particle layer becomes significant as the distance between particle surfaces falls below 50 Å. The surface potential will also give rise to a displacement force and torque that tend to influence the path of the particle as it moves in the computation cell.

The Monte-Carlo simulation generated realistic looking particle cluster and networks in the dispersion, failed however to reproduce the large low field susceptibility found experimentally in well dispersed MP systems.

The molecular-dynamic model Much of the Monte-Carlo work indicated the lack of knowledge of the detailed dispersion dynamics, specifically of the time-scale for the particle rotation, which is unobtainable from the MC approach. Consequently it was decided to develop a molecular dynamic (MD) simulation, which essentially involves a solution of the coupled equations of motion of all the particles in the ensemble. The most significant features of the molecular dynamic model relate to the first-order prediction of real-time dynamic behaviour of a particulate dispersion where the motion of each particle has been constrained via the interaction with a viscous medium.

This interaction has been simulated by introducing a force and torque that are derived from the motion of a single particle in a Newtonian fluid. Although this is a simplistic approach in regard to the general problem of viscous flow, it is expected to approximate the constraint on the motion of a particle due to the dispersion medium and consequently allow events to scale to within a reasonable order of magnitude of real time. This gives rise to the possibility of studying dynamic behaviour and correlating predictions with experiment.

After concern about the assumption of Newtonian **behaviour** rheological measurements were undertaken by **Anacomp** which suggest that the Newtonian approximation is in fact a reasonable first-order assumption.

The first MD simulation employed the usual forms of the equations of motion known as the velocity Verlet and the rotational leapfrog algorithms. Instabilities arose due to the over-estimation of the velocity during a given time step causing problems with the velocity dependent viscous forces and torques. Rather than accept an unreasonably small time-step in order to stabilise the algorithms, a new set was developed incorporating an analytical description of the particle motions while neglecting initial effects.

The simulation of the initial magnetisation curves provide a good comparison with experimental observation. **Very** satisfactory agreement was reached (figure 19) between theory and experiment for an advanced MP dispersion of very small particles.

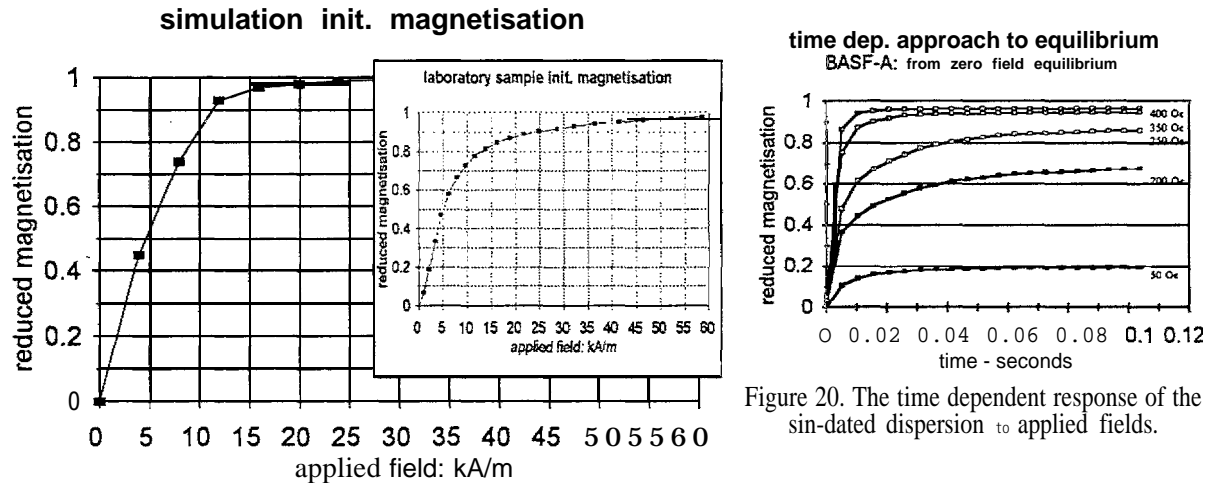


Figure 20. The time dependent response of the sin-dated dispersion to applied fields.

Figure 19. The MD simulation of the initial magnetisation curve.

The MD simulation was also found to be time dependent, with magnetisation changes taking place on a realistic **timescale** in comparison with experiment. An example relating the predicted time-dependent **behaviour** to real time is shown in figure 20. The low and high **fields** attain equilibrium relatively quickly. It is conjectured that the particle interactions are strong enough to constrain the particles in the low field case and the effect of the applied field dominates in the high field case. The mid field values are found to be slower to attain a stable particle **configuration** due to the fact that neither of these **two** effects is dominant and thus the local field of a particle is sensitive to the ensemble **configuration** on the approach to equilibrium. When combine with the new time dependence results expected from the UCNW impulse magnetometer the model should be the first capable of a realistic simulation of the orientation process and so be a tool in designing orientation systems.

Conclusions

From a wide range of potential methods devised at the beginning of this research three important practical techniques have evoked. The detailed theoretical treatment of dispersion filtering has produced a practical way of studying the **larger** agglomerates in experimental dispersions, Shear **magnetometry** has proven both a sources of **fundamental** data about the state of dispersion and especially about the function of kneading and a **practical** way of monitoring kneaded dispersions. The impulse magnetometer opens up a new range of time dependence measurements, which coupled with the simulation model can be used to optimize the design of orienting systems as well as give **information** about the state of agglomeration of the dispersions. Recently there is now **tremendous** interest-in very thin (0.1-0.3 μm) MP coatings for new recording **systems**. Using the dispersion model it has therefore become feasible to model the complete coating thickness as in a single cell with two rather than three dimensional repetition. **Modelling** the orienting, and drying, at first just as shrinkage, it will be possible to simulate the coating process to produce realistic starting points for calculations of ultimate surface roughness and media noise.

All the partners in project are actively applying and improving the methods described here.

Acknowledgements

This project was supported by the European Community **Brite/Euram** Programme, as Project BE5132 under contract BRE2-CT92-0157.

References

- [1] P. C. Scholten and J.A.P. Felijs, *J. Magn. Magn. Mat.*, vol. 80, pp.107-113,1990.
- [2] P. Scholten, "Magnetic particles in a liquid medium", in *Magnetic properties of fine particles*, J.L. Dormann and D. Fiorani, eds., North-Holland, 1992.
- [3] A.R. Balkenende, "Microstructure of magnetic dispersions studied by vibrating sheared sample magnetometry" *J. Magn. Magn. Mat.*, vol. 129, pp. 393-409, 1994.
- [4] H.P. Huisman and H.J.M. Pigmans, " Dispersion of magnetic pigments III. A kneader investigation", *J. Disper. Sci. Techn.*, vol. 7, pp. 187-213, 1986.
- [5] H.P. Grace, "Structure and Performance of Filter Media" *J.A.I. Chem.E.* 2,307, (1956).
- [6] M Kudo, N. Nagasaki, T. Masuko, "Evaluation for the dispersed state of magnetic paints containing Ba ferrite fine particles by constant pressure method". *Shikizai Kyokaiishi* (Journal of the Japan Society of Colour Material), 69,83, (1996), Japanese language.
- [7] P.C.Carmen, "**Determination** of the Specific Surface of Powders IT' *J. Sot. Chem. Ind.* (London) 58,1-7, (1939), Also Hatch L.P., *Trans. Am. Geophysics Union* 24,(1943).